POTSDAM-INSTITUT FÜR
KLIMAFOLGENFORSCHUNG

PIK

Originally published as:

Climate simulations of Neoproterozoic snowball Earth events: Similar critical carbon dioxide levels for the Sturtian and Marinoan glaciations

Georg Feulner & Hendrik Kienert

Earth System Analysis, Potsdam Institute for Climate Impact Research, P.O. Box 60 12 03, D–14412 Potsdam, Germany

Abstract

The Sturtian and Marinoan snowball Earth episodes initiated 720 and 650 million years ago, respectively, are among the most dramatic events in Earth's history. The ultimate causes of these events remain obscure, however, and there is still uncertainty about the critical levels of greenhouse gas concentrations at which the snowball transition occurs. Furthermore, earlier modelling results (with incomplete representations of important boundary conditions) provided conflicting indications for differences between the critical carbon dioxide concentrations for the Marinoan and the Sturtian, reporting either the earlier or the later epoch to be more susceptible to global glaciation. Both the absolute values of and possible differences between these glaciation thresholds have profound implications for scenarios of snowball initiations during the Neoproterozoic. Here, we present coupled climate simulations (using an ocean general circulation model with dynamic/thermodynamic sea ice coupled to a fast atmosphere) focussing on the differences between the Neoproterozoic glaciations. For the first time, our simulations use realistic boundary conditions in terms of changes in solar luminosity between the two epochs and the most recent continental reconstructions. In agreement with previous studies with models including ocean and sea-ice dynamics, we report low values for the critical carbon dioxide concentration during the Neoproterozoic. But in contrast to hints from earlier studies we find very similar values of 100–130 ppm for the snowball bifurcation point during the Sturtian and Marinoan. This highlights the importance of realistic boundary conditions for climate simulations of the Neoproterozoic glaciations.

Keywords: snowball Earth bifurcation, Neoproterozoic climate, paleoclimate modeling, global glaciation, Rodinia breakup

1. Introduction

Episodes of global glaciation are certainly among the most dramatic events in Earth's climate history. The geologic record shows evidence for several periods of time with continental ice sheets in the tropics (Hoffman and Schrag, 2002), possibly implying oceans completely covered by ice.

The two most recent of these 'snowball Earth' events (Kirschvink, 1992) happened during the Neoproterozoic era (1000–541 Ma, 1 Ma = 1 million years ago) in a geologic period aptly called the Cryogenian (850–635 Ma). They are commonly referred to as the Sturtian and Marinoan glaciations and occurred about 720–700 Ma and 650–635 Ma, respectively (Macdonald et al., 2010).

From the point of view of Earth's energy balance, climate states with a completely frozen ocean surface appear to be a consequence of a fundamental instability caused by the positive ice-albedo feedback: increasing ice cover in a colder world results in a higher albedo and hence more solar radiation being reflected back into space, thus leading to further cooling. At some critical point, termed the snowball Earth bifurcation, the climate system rapidly moves into a stable state characterised by global ice cover. While the ice-albedo feedback has been discussed for a long time (Croll, 1867), the snowball instability is known since the time of the first energy balance model studies of glaciations (Öpik, 1965; Eriksson, 1968; Budyko, 1969;

Sellers, 1969). It is tempting to regard the geological evidence for low-latitude glaciations as manifestations of this fundamental climate instability, and the questions arise whether snowball Earth states can be simulated in climate models more sophisticated than the simple energy balance models, and, if yes, at which point they occur.

The study of these fascinating snowball Earth events has attracted considerable attention during the last two decades, and climate models spanning a wide range in complexity have been used to investigate this problem (e.g. Crowley, 1983; Jenkins, 1999; Chandler and Sohl, 2000; Hyde et al., 2000; Lewis et al., 2003; Donnadieu et al., 2004; Abbot et al., 2011; Pierrehumbert et al., 2011; Voigt et al., 2011; Liu et al., 2013). Three key questions arising from climate model studies of the Neoproterozoic are the focus of ongoing debates. First, at which critical greenhouse gas concentration (for a given Neoproterozoic solar constant) does the climate system enter a snowball state, and is this concentration higher than reasonably expected for that time period as some models indicate? Second, what is the difference between the critical CO_2 levels for the Sturtian and the Marinoan? And third, is there an additional stable state with a narrow belt of open water around the equator (sometimes called 'soft snowball' or 'slushball') rather than the global ice cover of a 'hard snowball'? These issues are of obvious relevance for the most fundamental of all questions: What triggered the Neoproterozoic glaciations in the first place?

Concerning the critical CO_2 concentration, a recent model intercomparison exercise shows that atmospheric general circulation models (AGCMs) coupled to a mixed-layer ocean with zero heat transport enter a snowball state between 1000 and 6000 ppm of CO_2 for a present-day continental configuration and a solar constant of $1285\,W/m^2$, while a coupled atmosphere-ocean general circulation model (AOGCM) yields a considerably lower value between 286 ppm and 572 ppm of CO_2 (Pierrehumbert et al., 2011; Voigt et al., 2011). The authors reasonably attribute this difference to the lack of ocean heat transport in the AGCM simulations. The generally lower values in models with ocean dynamics are confirmed by a recent study by Liu et al. (2013) who report critical CO_2 values even lower than Voigt et al. (2011), most likely due to the more realistic lower albedo values used in Liu et al. (2013).

Possible differences between the Sturtian and Marinoan snowball bifurcation points could shed some light on the ultimate causes of global glaciations. This is particularly relevant for hypotheses depending on continental configuration such as those suggesting enhanced drawdown of atmospheric CO_2 by weathering of tropical continents (Hoffman and Schrag, 2002) or flood basalts (Goddéris et al., 2003). Few studies, however, investigate (or touch upon) potential differences between the Sturtian and the Marinoan. Lewis et al. (2003) use an ocean general circulation model coupled to an energy-moisture balance atmosphere to study the influence of idealised continental configurations, finding that an equatorial supercontinent is more susceptible to global glaciation than supercontinents at higher latitudes. Voigt et al. (2011) report a cooling when moving from present-day conditions to the predominantly low-latitude continents in their AOGCM simulations for a Marinoan configuration. These two studies would thus indicate higher critical CO_2 levels for the Sturtian because of its low-latitude continents. Other studies with comparatively simple models, however, find that states with higher-latitude continents (Crowley, 1983) or more dispersed continental configurations (Donnadieu et al., 2004) are characterised by higher critical CO_2 concentrations than those with an equatorial supercontinent. This seems to be confirmed by a recent AOGCM study (Liu et al., 2013) which indicates that a 570 Ma continental configuration (taken to represent the Marinoan in that paper) is more susceptible to glaciation than a Sturtian configuration. However, most of these studies are based on idealised continental configurations, and none of them takes into account the non-negligible changes in solar luminosity between the Sturtian and the Marinoan.

Soft snowball states with comparatively narrow belts of open water around the equator appear attractive because they can easily explain the survival of photosynthetic life through extended snowball periods. To be consistent with the geologic record, low-latitude continental ice would have to exist in such states. Soft snowball states are reported in a number of modelling studies (Hyde et al., 2000; Liu and Peltier, 2010; Abbot et al., 2011). Most models which include ocean and sea-ice dynamics show no evidence for soft snowball states (Lewis et al., 2003; Voigt and Abbot, 2012) – with the exception of Yang et al. (2012), indicating that these effect tend to destabilise soft snowball states.
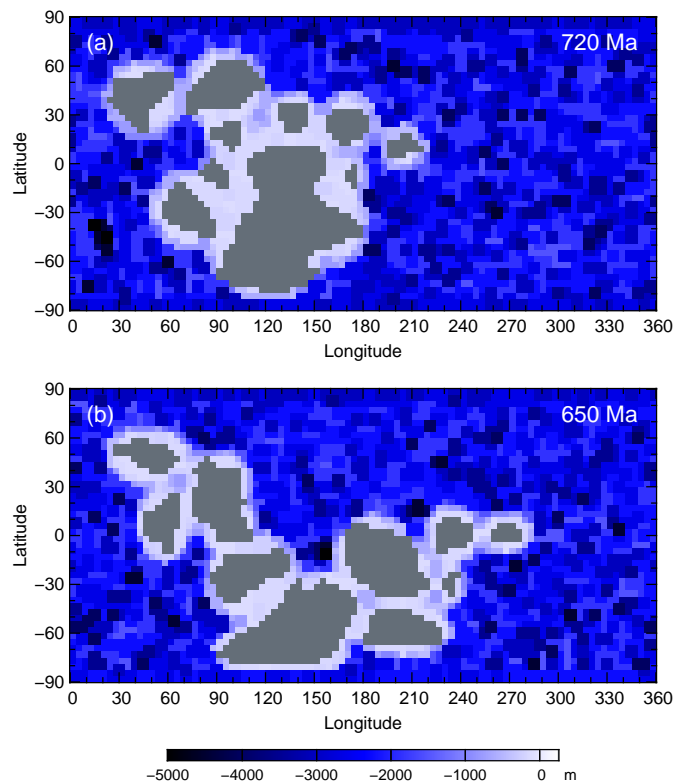
Figure 1: Neoproterozoic continental configurations and ocean depth levels used for simulating the (a) Sturtian and (b) Marinoan glaciations.

However, the small number of such modelling studies, the considerable variations between different models and the lack of AOGCM studies with a coupled continental ice-sheet model preclude a final verdict on the existence of soft snowball states.

Here we explore the Neoproterozoic snowball Earth episodes using an ocean general circulation model including a dynamic/thermodynamic sea-ice model coupled to a fast atmosphere model. We investigate the critical carbon dioxide concentration and relate it to earlier results obtained with AGCMs coupled to a mixed-layer ocean and full AOGCMs, with a particular focus on possible differences between the Sturtian and Marinoan glaciations. Our work is based on the first coupled climate model simulations using appropriate boundary conditions in terms of the most recent reconstruction of Neoproterozoic continental configurations and taking into account the change in solar constant between the two events which had previously been neglected.

This paper is organised as follows. In Section 2, we describe the model as well as the boundary conditions used for our simulations. Section 3 discusses the critical carbon dioxide concentrations for the Sturtian and the Marinoan glaciations. Finally, Section 4 summarises our results.

2

2. Model setup and experiments

2.1. Model description

For our simulations we use an ocean general circulation model including sea ice coupled to a fast atmosphere model (Montoya et al., 2006). The ocean model (the Modular Ocean Model MOM3, Pacanowski and Griffies 1999) is operated at a relatively low horizontal resolution of 3.75°×3.75° with 24 vertical layers. The sea-ice model (Fichefet and Morales Maqueda, 1997) captures both the thermodynamics and the dynamics of sea ice. The fast atmosphere model does not solve the primitive equations, but statistically describes the large-scale circulation patterns and their dynamical response to climate changes (Petoukhov et al., 2000). It is employed at a horizontal resolution of 22.5° in longitude and 7.5° in latitude with 16 vertical layers.

It is important to note that the model realistically simulates ocean heat transport (which is suspected to explain the differences between atmospheric and coupled models of the Neoproterozoic, Pierrehumbert et al. 2011) and sea-ice dynamics (which has been shown to be important for studying the snowball bifurcation, Voigt and Abbot 2012) while being sufficiently fast computationally to allow for a relatively large number of ensemble simulations.

The model has previously been used in a large number of studies including several model intercomparison projects (Gregory et al., 2005; Stouffer et al., 2006; Jansen et al., 2007; Eby et al., 2013; Zickfeld et al., 2013). Here, in contrast to the simulations of the faint young Sun paradox (Feulner, 2012) presented in Kienert et al. (2012, 2013), we use a model version with an improved parameterisation of the atmospheric lapse rate (see Appendix A) and lower clear-sky albedo values of 0.50 and 0.40 for freezing and melting sea-ice, and 0.75 and 0.65 for cold and warm snow, respectively. The model distinguishes between visible and near-infrared albedos by assuming partitions of 60% and 40% for these bands and assigning 0.30 larger values for the optical albedos. The effects of snow cover on sea-ice are taken into account.

2.2. Neoproterozoic boundary conditions

2.2.1. Continental configuration

While there is still considerable uncertainty about the distribution of continents during the Neoproterozoic, the fundamental characteristics agree between different reconstructions. In general, the Neoproterozoic continental distribution reflects the breakup of the supercontinent Rodinia after about 750 Ma. The continental configurations for the Sturtian and Marinoan time periods used in our model experiments are shown in Figure 1. They are based on the most recent reconstructions from Li et al. (2013) for the 720 Ma and 635 Ma time slices, respectively. The Sturtian continental distribution is characterised by the onset of the Rodinia breakup with relatively tightly packed fragments roughly symmetrical about the equator. During the Marinoan, however, the continental pieces are more widely dispersed in an elongated form mostly concentrated in the Southern hemisphere.

For our simulations, the reconstructed emerged continental areas are artificially surrounded by continental shelf cells with shallower ocean depth of up to ∼ 400 m and adjacent continental slope regions with depth levels up to ∼ 1200 m. All other ocean cells are assigned deep ocean depth values of up to ∼ 5500 m. Depth values for all ocean grid cells are assigned randomly in a way which ensures that the total ocean volume is similar to the one today. Land elevation is set to a uniform level of 250 m. All land areas are set to be free of vegetation and to have an albedo of 0.14 in the optical unless covered by snow.

2.2.2. Solar constant and orbital parameters

We calculate the solar constant at the time of the Neoproterozoic glaciations based on the standard solar model results published in Bahcall et al. (2001) and assuming a present-day value of 1361 W/m^2 (Kopp and Lean, 2011). For the onset of the Sturtian and Marinoan glaciations 720 Ma and 650 Ma, this approach results in values of 1283 W/m^2 and 1290 W/m^2, respectively. All model simulations use an idealised orbital configuration with a circular orbit and an obliquity of 23.5°.

2.3. Model experiments

For each of the two Neoproterozoic snowball Earth episodes we run model simulations with the appropriate continental configuration and solar constant, and with a wide range of CO_2 concentrations (from 100 ppm to 9000 ppm) to pinpoint the snowball bifurcation. The concentrations of other greenhouse gases (except water vapour, of course) are assumed to be zero. All model simulations are initiated from an ice-free ocean state with constant present-day salinity and a smoothed sea-surface temperature profile which is symmetrical about the equator and approximates modern ocean observations. All experiments are integrated for 2000 model years until equilibrium is approached. The two critical state simulations discussed below are run for an additional period of 30 years to obtain climatologies for all variables. All diagnostics are computed for the last 30 years of each run.

3. The snowball bifurcation for the Sturtian and Marinoan glaciations

Global and annual mean surface air temperatures as a function of atmospheric carbon-dioxide concentration for the Sturtian and Marinoan are displayed in Figure 2. The insets show the annual mean sea-ice fraction for the critical states of both time-slices; sea-ice thickness and velocities are shown in Figure 3. In both cases the snowball bifurcation occurs between 100 ppm and 130 ppm of CO_2 in our model. For the Sturtian, the coldest stable state is characterised by a CO_2 concentration of 110 ppm and has a global and annual mean surface air temperature of 266 K (−7.0°C), while a state with 100 ppm of CO_2 is fully glaciated. For the Marinoan, the coldest state with ice-free ocean regions has 130 ppm of CO_2 and 268 K (−4.8°C) global temperature; reducing CO_2 to 120 ppm leads to a snowball state. Climate sensitivity with respect to doubling of CO_2 increases with decreasing temperature from ∼3.4 K for

the warm states (identical to the present-day sensitivity of the model, Feulner and Rahmstorf 2010) to ~6 K close to the snowball bifurcation (in good agreement with the value reported in Liu et al. 2013). We do not see evidence for soft snowball states in our simulations. Since we do not explicitly model continental ice sheets, however, this does not necessarily imply that states with open ocean areas and low-latitude ice-sheets cannot exist.

Our critical CO_2 concentrations for the Sturtian and Marinoan appear to be in good agreement with the 80–90 ppm and 140–150 ppm from AOGCM simulations with standard aerosol optical depth presented in Liu et al. (2013) considering the differences in solar constant and warming by other greenhouse gases. Compared to their simulations with lower optical depth, our values are somewhat higher. Both studies, however, yield lower values than Voigt et al. (2011) who report the bifurcation between 286 ppm and 572 ppm of CO_2 (plus 650 ppb of CH_4 and 270 ppb of NO_2) for a Marinoan continental configuration and a solar constant of 1285 W/m^2, a difference which is probably due to the higher sea-ice albedos assumed in Voigt et al. (2011). All of these studies consistently point to critical CO_2 concentrations considerably lower than derived using AGCMs coupled to a mixed-layer ocean without heat transport, emphasizing the critical role of oceanic heat transport processes for the snowball bifurcation (Pierrehumbert et al., 2011).
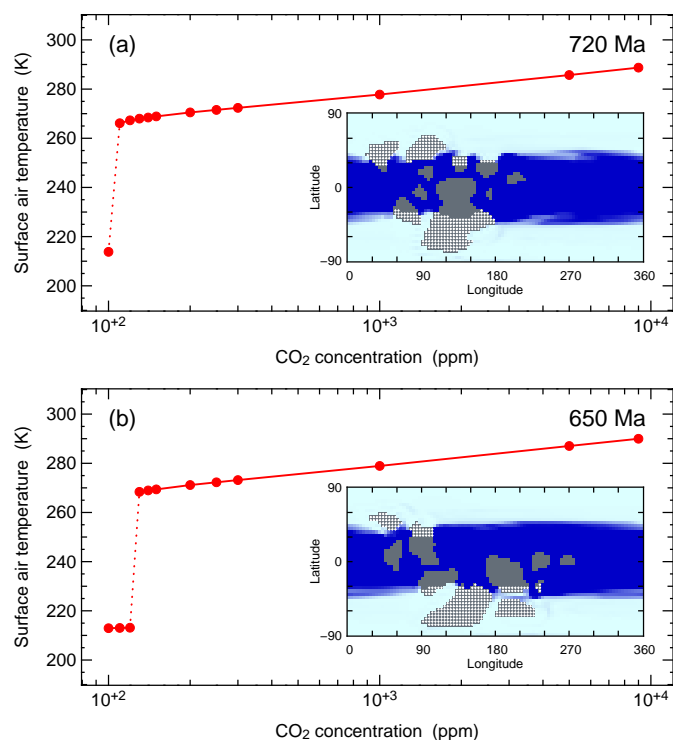
Figure 2: Global and annual average of surface air temperature as a function of atmospheric carbon dioxide concentration in our simulations for the Sturtian (a) and Marinoan (b). The insets show the sea-ice distribution for the coldest partially ice-covered state (110 ppm experiment for the Sturtian, 130 ppm for the Marinoan). White crosses indicate land areas with an annual mean snow fraction of at least 20%.

Interestingly, and in contrast to previous work discussed in Section 1, we find very similar values for the critical CO_2 concentration for the Sturtian and the Marinoan. In our simulations, the cooling due to the larger fraction of land at higher Southern latitudes in the Marinoan appears to be compensated by the increase in solar luminosity since the Sturtian.

To separate the effects of changes in continental configuration and solar luminosity, we perform additional simulations for the Marinoan using the lower solar constant value of the Sturtian. At the same solar constant of 1283 W/m^2 and CO_2 concentration of 200 ppm, the simulation for the Marinoan is about 1.5 K cooler than the one for the Sturtian, confirming the cooling effect of the higher fraction of high-latitude continents. Using the same Marinoan continental configuration and CO_2 concentration of 200 ppm, the simulation with a solar constant of 1290 W/m^2 is about 2.2 K warmer than the one with 1283 W/m^2, thus roughly compensating for the change due to continental configuration. Accordingly, the critical CO_2 concentration for the Marinoan neglecting the increase in solar luminosity would be 180 ppm rather than 130 ppm discussed above.

In the literature, the most comprehensive study of possible differences between the two Neoproterozoic glaciations is the study by Liu et al. (2013). That study, however, ignores the increase of solar luminosity between 720 Ma and 650 Ma, thus requiring higher CO_2 concentrations for their Marinoan simulation. Furthermore, their Marinoan continental configuration is more representative of later times (570 Ma) and characterised by an even higher fraction of land at high Southern latitudes, again overestimating the cooling due to changes in paleogeography.

Zonal averages of important physical diagnostics of the simulated critical climate states during the Sturtian and Marinoan are shown in Figure 4. Annual mean surface air temperature profiles of both states are very similar with temperatures around 280 K in the tropics and 230 K at the poles (Figure 4a). As expected from the continental configurations, the 720 Ma critical state has a symmetrical temperature profile, while the 650 Ma state with its landmasses at high Southern latitudes is slightly warmer in the Northern Hemisphere.

The planetary albedo reaches values between 0.25 and 0.30 in the ice-free tropics and between 0.70 and 0.75 in the sea-ice covered higher latitudes (Figure 4b). The planetary albedo profile is in good agreement with the AOGCM simulations presented in Liu et al. (2013). The overall values in our model appear to be somewhat higher, thus explaining the slightly higher critical CO_2 concentrations in our model compared to theirs.

As discussed above, ocean and sea-ice dynamics have a major influence on the sea-ice limit and thus the snowball bifurcation point. For both Neoproterozoic states, ocean heat transport has a similar structure as in the present-day climate system, but is more vigorous than today (Figure 4c), thus making global glaciation more difficult by transporting heat towards the ice margin. This highlights the importance of using ocean general circulation models for deep-time paleoclimate problems.

The same is true for sea-ice dynamics. The importance of sea-ice dynamics is already evident from the complicated structure of the annual-average ice margin in the critical states shown in Figure 2. Annual mean sea-ice thickness and velocity vectors
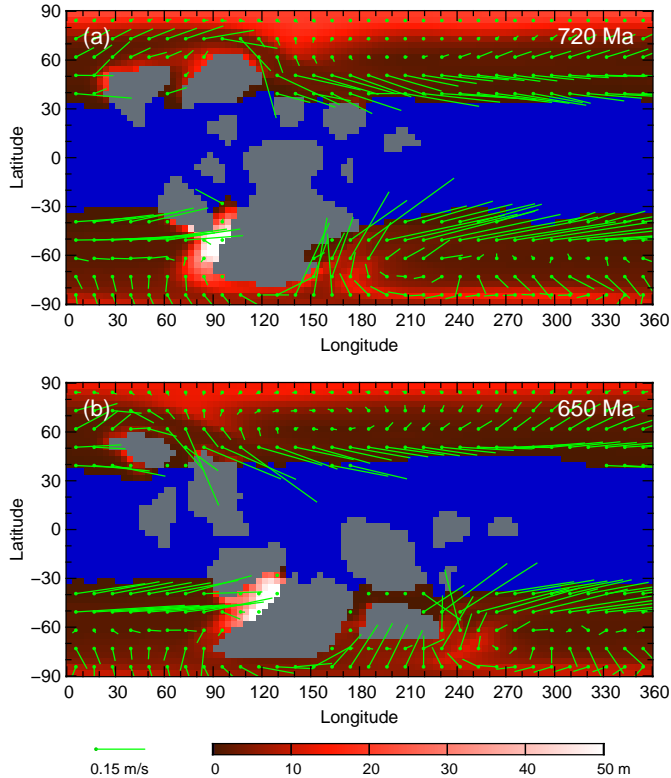
Figure 3: Annual average sea-ice thickness (red shading) and sea-ice velocity (green arrows) for the Sturtian (a) and Marinoan (b). In both cases the diagnostics are shown for the coldest partially ice-covered state (110 ppm experiment for the Sturtian, 130 ppm for the Marinoan).

are presented in Figure 3. In particular, there is considerable meridional drift of sea-ice towards the equator at intermediate latitudes as can be seen from Figure 4d. For the Northern Hemisphere in both epochs, we confirm earlier finding (Lewis et al., 2003; Liu et al., 2013) of strong sea-ice transport towards the equator induced by vigorous zonal flows in combination with the Coriolis force. In addition, however, we observe intense northward ice transport in the Southern hemisphere along the eastern boundaries of continents in both epochs (see Figure 3), resulting in the high northward zonal mean velocity of sea-ice in the Southern hemisphere apparent in Figure 4d. The influence of continental configuration on sea-ice dynamics thus significantly impacts the snowball Earth bifurcation point during the Neoproterozoic.

4. Conclusions

In this study, we have presented coupled climate simulations of the Neoproterozoic snowball Earth episodes during the Sturtian (720–700 Ma) and Marinoan (650–635 Ma) based on the most recent continental reconstructions. For the first time, changes in solar luminosity between these two epochs have been taken into account.

In agreement with previous work based on models capturing ocean and sea-ice dynamics, we find low values for the critical

atmospheric carbon-dioxide concentration at the snowball bifurcation. The absolute values are model dependent, our model yields a range of 100–130 ppm of CO_2. It should be noted that the simplified atmospheric dynamics in our model could affect the location of the snowball bifurcation point. The low values for the critical carbon-dioxide concentration are predominantly due to the vigorous meridional heat transport in the ocean. Furthermore, we find strong sea-ice motion towards the equator in the mid-latitudes caused by a combination of Ekman transport due to strong zonal flows in regions with little continental area and sea-ice drift along the eastern borders of continents. These findings emphasize the importance of ocean and sea-ice dynamics for the Neoproterozoic snowball bifurcation.

The larger fraction of continental area at higher Southern latitudes during the Marinoan leads to a cooling as compared to the Sturtian, making the Marinoan more prone to global glaciation in principle. In our simulations, this cooling is roughly compensated by the increase in solar luminosity between both epochs, however, resulting in very similar values for the critical CO_2 concentration at the snowball bifurcation point. It is therefore vital to take all boundary conditions into account when comparing the Neoproterozoic glaciations.

Appendix A. Lapse-rate parameterisation

For this study we use an improved parameterisation of the atmospheric lapse rate Γ as a function of surface-air temperature T_a, specific humidity q_s and cumulus cloud fraction n_c: $\Gamma = \Gamma_0 + \Gamma_1(T_a + 10\,K - 273.16\,K)(1 - a_q \times q_s^2) - \Gamma_2 n_c$ with parameters $\Gamma_0 = 5.0 \times 10^{-3}\,K\,m^{-1}$, $\Gamma_1 = 5.0 \times 10^{-5}\,m^{-1}$, $\Gamma_2 = 0$ and $a_q = 1111\,(kg/kg)^{-2}$. Although not explicitly stated in Montoya et al. (2006), this is the standard parameterisation used in all previously published papers using this model (except for Kienert et al. 2012, 2013), and its parameter values are slightly different from the ones chosen in Petoukhov et al. (2000) cited in Montoya et al. (2006). In contrast to this standard model version, and in order to improve the performance for cold climate states, the lower limit of the lapse rate is reduced from 3 K/km to 1 K/km for this study to better capture small values over cold polar regions, in particular in winter. In addition to giving a very good representation of the observed seasonal and geographical variations of the lapse rate under present-day climate conditions, the validity of these parameters for cold climate states is tested by comparison with results from simulations of early Earth's climate with an atmospheric general circulation model (Kunze et al., 2014) yielding good agreement.
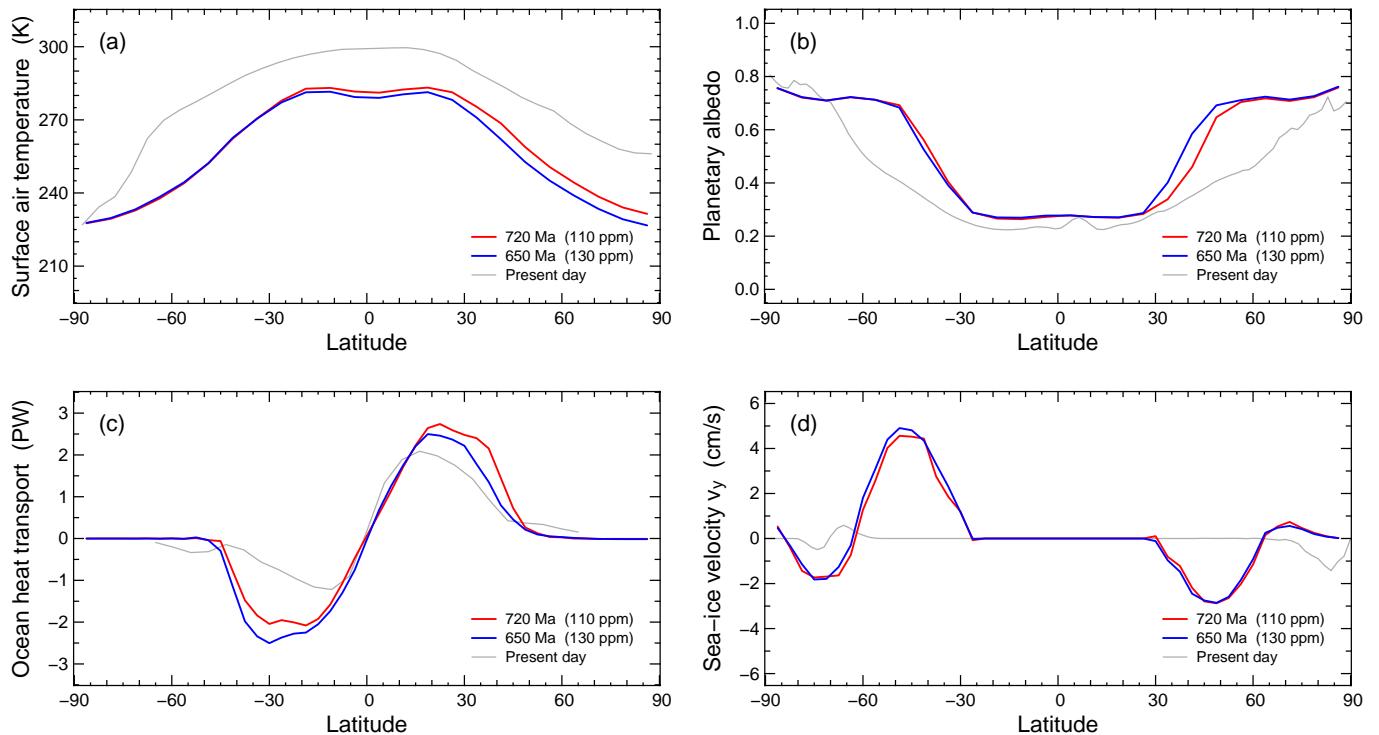
Figure 4: Comparison of physical characteristics of the critical states during the Sturtian (110 ppm of CO_2, blue) and Marinoan (130 ppm of CO_2, red) in relation to present-day observations (grey). (a) Annual and zonal mean surface air temperature (present-day observations for 1961–1990 from Jones et al. 1999). (b) Annual and zonal mean planetary albedo (present-day data for 2000–2004 from Fasullo and Trenberth 2008). (c) Meridional ocean heat transport (present-day estimate for 1985–1989 from Trenberth and Caron 2001). (d) Annual and zonal mean meridional sea-ice velocity (present-day data for 1992–2001 from Fowler et al. 2013, described in Maslanik et al. 2011).

References

Abbot, D. S., Voigt, A., Koll, D., Sep. 2011. The Jormungand global climate state and implications for Neoproterozoic glaciations. J. Geophys. Res. 116, 18103.

Bahcall, J. N., Pinsonneault, M. H., Basu, S., Jul. 2001. Solar Models: Current Epoch and Time Dependences, Neutrinos, and Helioseismological Properties. Astrophys. J. 555, 990–1012.

Budyko, M. I., 1969. The effect of solar radiation variations on the climate of the earth. Tellus 21, 611–619.

Chandler, M. A., Sohl, L. E., 2000. Climate forcings and the initiation of low-latitude ice sheets during the Neoproterozoic Varanger glacial interval. J. Geophys. Res. 105, 20737–20756.

Croll, J., 1867. XVII. On the excentricity of the Earth's orbit, and its physical relations to the glacial epoch. Philosophical Magazine Series 4 33 (221), 119–131.

Crowley, T. J., 1983. The Geologic Record of Climatic Change. Rev. Geophys. 21, 828–877.

Donnadieu, Y., Ramstein, G., Fluteau, F., Roche, D., Ganopolski, A., 2004. The impact of atmospheric and oceanic heat transports on the sea-ice-albedo instability during the Neoproterozoic. Clim. Dynam. 22, 293–306.

Eby, M., Weaver, A. J., Alexander, K., Zickfeld, K., Abe-Ouchi, A., Cimatoribus, A. A., Crespin, E., Drijfhout, S. S., Edwards, N. R., Eliseev, A. V., Feulner, G., Fichefet, T., Forest, C. E., Goosse, H., Holden, P. B., Joos, F., Kawamiya, M., Kicklighter, D., Kienert, H., Matsumoto, K., Mokhov, I. I., Monier, E., Olsen, S. M., Pedersen, J. O. P., Perrette, M., Philippon-Berthier, G., Ridgwell, A., Schlosser, A., Schneider von Deimling, T., Shaffer, G., Smith, R. S., Spahni, R., Sokolov, A. P., Steinacher, M., Tachiiri, K., Tokos, K., Yoshimori, M., Zeng, N., Zhao, F., May 2013. Historical and idealized climate model experiments: an intercomparison of Earth system models of intermediate complexity. Clim. Past 9, 1111–1140.

Eriksson, E., 1968. Air-ocean-icecap interactions in relation to climatic fluctuations and glaciation cycles. Meteorological Monographs 8, 68–92.

Fasullo, J. T., Trenberth, K. E., 2008. The Annual Cycle of the Energy Budget. Part I: Global Mean and Land-Ocean Exchanges. J. Climate 21, 2297–2312.

Feulner, G., 2012. The faint young sun problem. Rev. Geophys. 50, RG2006.

Feulner, G., Rahmstorf, S., Mar. 2010. On the effect of a new grand minimum of solar activity on the future climate on Earth. Geophys. Res. Lett. 37, L05707.

Fichefet, T., Morales Maqueda, M. A., 1997. Sensitivity of a global sea ice model to the treatment of ice thermodynamics and dynamics. J. Geophys. Res. 102, 12609–12646.

Fowler, C., Emery, W., Tschudi, M., 2013. Polar Pathfinder Daily 25 km EASE-Grid Sea Ice Motion Vectors. Version 2. National Snow and Ice Data Center Boulder, Colorado USA. Distributed in netCDF format by the Integrated Climate Data Center (ICDC, http://icdc.zmaw.de) University of Hamburg, Hamburg, Germany.

Goddéris, Y., Donnadieu, Y., Nédélec, A., Dupré, B., Dessert, C., Grard, A., Ramstein, G., François, L. M., Jun. 2003. The Sturtian 'snowball' glaciation: fire and ice. Earth and Planetary Science Letters 211, 1–12.

Gregory, J. M., Dixon, K. W., Stouffer, R. J., Weaver, A. J., Driesschaert, E., Eby, M., Fichefet, T., Hasumi, H., Hu, A., Jungclaus, J. H., Kamenkovich, I. V., Levermann, A., Montoya, M., Murakami, S., Nawrath, S., Oka, A., Sokolov, A. P., Thorpe, R. B., Jun. 2005. A model intercomparison of changes in the Atlantic thermohaline circulation in response to increasing atmospheric CO_2 concentration. Geophys. Res. Lett. 32, 12703.

Hoffman, P. F., Schrag, D. P., 2002. The snowball Earth hypothesis: testing the limits of global change. Terra Nova 14, 129–155.

Hyde, W. T., Crowley, T. J., Baum, S. K., Peltier, W. R., May 2000. Neoproterozoic 'snowball Earth' simulations with a coupled climate/ice-sheet model. Nature 405, 425–429.

Jansen, E., Overpeck, J., Briffa, K. R., Duplessy, J.-C., Joos, F., Masson-Delmotte, V., Olago, D., Otto-Bliesner, B., Peltier, W. R., Rahmstorf, S., Ramesh, R., Raynaud, D., Rind, D., Solomina, O., Villalba, R., Zhang, D., 2007. Palaeoclimate. In: Solomon, S., Qin, D., Manning, M., Chen, Z., Marquis, M., Averyt, K., Tignor, M., Miller, H. (Eds.), Climate Change 2007: The Physical Science Basis. Cambridge Univ. Press, Cambridge, U.K. and

New York, NY, USA.

Jenkins, G. S., May 1999. Examining the sensitivity of Earth's climate to the removal of ozone, landmasses and enhanced ocean heat transport in the GENESIS global climate model. Global Planet. Change 20, 257–279.

Jones, P. D., New, M., Parker, D. E., Martin, S., Rigor, I. G., 1999. Surface air temperature and its changes over the past 150 years. Rev. Geophys. 37, 173–200.

Kienert, H., Feulner, G., Petoukhov, V., Dec. 2012. Faint young Sun problem more severe due to ice-albedo feedback and higher rotation rate of the early Earth. Geophys. Res. Lett. 39, 23710.

Kienert, H., Feulner, G., Petoukhov, V., 2013. Albedo and heat transport in 3-D model simulations of the early Archean climate. Clim. Past 9, 1841–1862.

Kirschvink, J. L., 1992. Late Proterozoic Low-Latitude Global Glaciation: the Snowballl Earth. In: Schopf, J. W., Klein, C. (Eds.), The Proterozoic Biosphere: A Multidisciplinary Study. Cambridge University Press, Cambridge, pp. 51–52.

Kopp, G., Lean, J. L., 2011. A new, lower value of total solar irradiance: Evidence and climate significance. Geophys. Res. Lett. 38, L01706.

Kunze, M., Godolt, M., Langematz, U., Grenfell, J. L., Hamann-Reinus, A., Rauer, H., 2014. Investigating the Early Earth Faint Young Sun Problem with a General Circulation Model. Planet. Space Sci. 98, 77–92.

Lewis, J. P., Weaver, A. J., Johnston, S. T., Eby, M., Dec. 2003. Neoproterozoic "snowball Earth": Dynamic sea ice over a quiescent ocean. Paleoceanography 18, 1092.

Li, Z.-X., Evans, D. A., Halverson, G., 2013. Neoproterozoic glaciations in a revised global palaeogeography from the breakup of rodinia to the assembly of gondwanaland. Sediment. Geol. 294, 219–232.

Liu, Y., Peltier, W. R., Sep. 2010. A carbon cycle coupled climate model of Neoproterozoic glaciation: Influence of continental configuration on the formation of a "soft snowball". J. Geophys. Res. 115, 17111.

Liu, Y., Peltier, W. R., Yang, J., Vettoretti, G., Nov. 2013. The initiation of Neoproterozoic "snowball" climates in CCSM3: the influence of paleocontinental configuration. Clim. Past 9, 2555–2577.

Macdonald, F. A., Schmitz, M. D., Crowley, J. L., Roots, C. F., Jones, D. S., Maloof, A. C., Strauss, J. V., Cohen, P. A., Johnston, D. T., Schrag, D. P., Mar. 2010. Calibrating the Cryogenian. Science 327, 1241–1243.

Maslanik, J., Stroeve, J., Fowler, C., Emery, W., Jul. 2011. Distribution and trends in Arctic sea ice age through spring 2011. Geophys. Res. Lett. 38, 13502.

Montoya, M., Griesel, A., Levermann, A., Mignot, J., Hofmann, M., Ganopolski, A., Rahmstorf, S., Feb. 2006. The earth system model of intermediate complexity CLIMBER-3α. Part I: description and performance for present-day conditions. Clim. Dynam. 26, 327–328.

Öpik, E. J., Jul. 1965. Climatic Change in Cosmic Perspective. Icarus 4, 289–307.

Pacanowski, R. C., Griffies, S. M., 1999. The MOM-3 Manual. Tech. Rep. 4, GFDL Ocean Group, NOAA/Geophysical Fluid Dynamics Laboratory, Princeton, NJ.

Petoukhov, V., Ganopolski, A., Brovkin, V., Claussen, M., Eliseev, A., Kubatzki, C., Rahmstorf, S., 2000. CLIMBER-2: a climate system model of intermediate complexity. Part I: model description and performance for present climate. Clim. Dynam. 16, 1–17.

Pierrehumbert, R. T., Abbot, D. S., Voigt, A., Koll, D., May 2011. Climate of the Neoproterozoic. Annu. Rev. Earth Pl. Sc 39, 417–460.

Sellers, W. D., Jun. 1969. A Global Climatic Model Based on the Energy Balance of the Earth-Atmosphere System. J. Appl. Meteorol. 8, 392–400.

Stouffer, R. J., Yin, J., Gregory, J. M., Dixon, K. W., Spelman, M. J., Hurlin, W., Weaver, A. J., Eby, M., Flato, G. M., Hasumi, H., Hu, A., Jungclaus, J. H., Kamenkovich, I. V., Levermann, A., Montoya, M., Murakami, S., Nawrath, S., Oka, A., Peltier, W. R., Robitaille, D. Y., Sokolov, A., Vettoretti, G., Weber, S. L., 2006. Investigating the Causes of the Response of the Thermohaline Circulation to Past and Future Climate Changes. J. Climate 19, 1365.

Trenberth, K. E., Caron, J. M., Aug. 2001. Estimates of Meridional Atmosphere and Ocean Heat Transports. J. Climate 14, 3433–3443.

Voigt, A., Abbot, D. S., Dec. 2012. Sea-ice dynamics strongly promote Snowball Earth initiation and destabilize tropical sea-ice margins. Clim. Past 8, 2079–2092.

Voigt, A., Abbot, D. S., Pierrehumbert, R. T., Marotzke, J., Mar. 2011. Initiation of a Marinoan Snowball Earth in a state-of-the-art atmosphere-ocean general circulation model. Clim. Past 7, 249–263.

Yang, J., Peltier, W. R., Hu, Y., Apr. 2012. The Initiation of Modern "Soft Snowball" and "Hard Snowball" Climates in CCSM3. Part I: The Influences of Solar Luminosity, CO2Concentration, and the Sea Ice/Snow Albedo Parameterization. J. Climate 25, 2711–2736.

Zickfeld, K., Eby, M., Weaver, A. J., Alexander, K., Crespin, E., Edwards, N. R., Eliseev, A. V., Feulner, G., Fichefet, T., Forest, C. E., Friedlingstein, P., Goosse, H., Holden, P. B., Joos, F., Kawamiya, M., Kicklighter, D., Kienert, H., Matsumoto, K., Mokhov, I. I., Monier, E., Olsen, S. M., Pedersen, J. O. P., Perrette, M., Philippon-Berthier, G., Ridgwell, A., Schlosser, A., Schneider Von Deimling, T., Shaffer, G., Sokolov, A., Spahni, R., Steinacher, M., Tachiiri, K., Tokos, K. S., Yoshimori, M., Zeng, N., Zhao, F., Aug. 2013. Long-Term Climate Change Commitment and Reversibility: An EMIC Intercomparison. J. Climate 26, 5782–5809.